Supporting Information for

Synthetic Versatility, Reaction Pathway, and Thermal Stability of Tetrahedrite Nanoparticles

Christine D. Fasana,† Mitchel S. Jensen,† Graciela E. García Ponte,† Tyler R. MacAlister,† Grace E. Kunkel,‡ John P. Rogers,‡ Andrew M. Ochs,‡ Daniel L. Stevens,‡ Daniel P. Weller,* Donald T. Morelli,* Mary E. Anderson†

† Chemistry Department, Furman University, Greenville, SC

‡ Chemistry Department, Hope College, Holland, MI

* Chemical Engineering and Materials Science Department, Michigan State University, East Lansing, MI

Included:

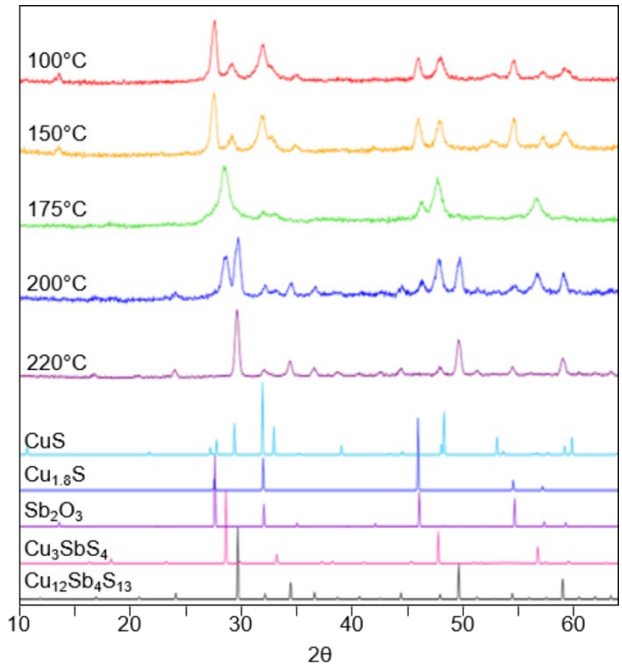

SI Figure 1. XRD patterns collected for Zn-doped tetrahedrite samples synthesized at different reaction temperatures. Reference patterns provided for tetrahedrite ($Cu_{12}Sb_4S_{13}$), famatinite (Cu_3SbS_4), digenite ($Cu_{1.8}S$), valentinite (Sb_2O_3), and covellite (CuS).

Table S1: Calculated Lattice Constant (a) for Tetrahedrite Compositions

Target Composition	a (Å)
$Cu_{12}Sb_4S_{13}$	10.389
$Cu_{10}Zn_2Sb_4S_{13}$	10.475
$Cu_{10.5}Zn_{1.5}Sb_4S_{13}$	10.475
$Cu_{11}ZnSb_4S_{13}$	10.455
$Cu_{11.5}Zn_{0.5}Sb_4S_{13}$	10.448
$Cu_{10}Ni_2Sb_4S_{13}$	10.413
$Cu_{11}NiSb_4S_{13}$	10.420
$Cu_{10}Co_2Sb_4S_{13}$	10.444
$Cu_{11}CoSb_4S_{13}$	10.430
$Cu_{10}Fe_2Sb_4S_{13}$	10.472
$Cu_{11}FeSb_4S_{13}$	10.430
$Cu_{10}Ag_2Sb_4S_{13}$	10.444
$Cu_{11}AgSb_4S_{13}$	10.455
$Cu_{12}Sb_{3.8}Te_{0.2}S_{13}$	10.410
$Cu_{12}Sb_4Se_{0.25}S_{12.75}$	10.403
$Cu_{11}ZnSb_4SeS_{13}$	10.510

Table S1 provides the lattice constant (a) for each composition of tetrahedrite (cubic structure) calculated from d_{hkl} and the Miller indices.

Bragg's law: $2d\sin\theta = n\lambda$

was used to find the interatomic spacing (d_{hkl}) based on the most intense peak at ~30 degrees, which is (222). The interatomic spacing (d_{hkl}) for a cubic system was calculated by the following:

$$d_{hkl} = \frac{a}{\sqrt{h^2 + k^2 + l^2}}$$

where a is the lattice constant and (hkl) are the Miller indices for a given plane.

Table S2: Atomic Mass % Range for $Cu_{12-14.5}Sb_{4-4.5}S_{13}$

	Cu	Sb	S
Target	41-46%	13-15%	41-43%

Table S2 is provided for reference to Table S3 and S4, these are the ranges for the atomic mass percentages based on the elemental range of tetrahedrite compositions: $Cu_{12-14.5}Sb_{4-4.5}S_{13}$.

Table S3: Average Atomic Mass % (based on EDS) as a function of Reaction Temperature

	Cu		Sb		S	
Temp (°C)	**avg (%)**	**stdev (%)**	**avg (%)**	**stdev (%)**	**avg (%)**	**stdev (%)**
25	48.7	3.2	15.1	2.0	36.1	1.2
100	52.2	3.6	8.3	3.1	39.6	2.9
150	46.7	2.8	14.66	0.54	38.6	3.0
175	51.9	3.1	9.42	0.61	38.7	2.8
200	49.23	0.77	7.66	0.17	43.18	0.88
215	48.1	1.7	10.04	0.30	41.9	1.4
220	45.15	0.53	13.60	0.59	41.25	0.09
250	49.6	3.1	14.35	0.43	36.1	3.1

Shown in Table S3 is energy-dispersive x-ray spectroscopy (EDS) quantitative analysis used to investigate the reaction pathway for the bottom-up solution-phase synthesis of tetrahedrite ($Cu_{12-14.5}Sb_{4-4.5}S_{13}$). The mass percentages of the resulting nanoparticle powders formed at these reaction temperatures after 60 minutes reaction time are shown in the table. A minimum of three spots were measured by EDS and the average of these measurements is given alongside the % stdev, which represents the spot-to-spot deviation.

Table S4: Average Atomic Mass % (based on EDS) as a function of Reaction Time

	Cu		Sb		S	
Time (min)	**avg (%)**	**stdev (%)**	**avg (%)**	**stdev (%)**	**avg (%)**	**stdev (%)**
1	43.87	0.83	15.24	0.66	40.9	1.2
30	51.3	8.5	12.9	1.2	35.8	7.4
60	45.15	0.53	13.60	0.59	41.247	0.088

Shown in Table S4 is EDS quantitative analysis used to investigate the reaction pathway for the bottom-up solution-phase synthesis of tetrahedrite ($Cu_{12\text{-}14.5}Sb_{4\text{-}4.5}S_{13}$). The mass percentages of the resulting nanoparticle powders formed after a specific reaction time listed in the chart at 220 °C. A minimum of three spots were measured by EDS and the average of these measurements is given alongside the % stdev, which represents the spot-to-spot deviation.